

Cryptotanshinone inhibits human glioma cell proliferation by suppressing STAT3 signaling

Liang Lu · Cuixian Li · Dong Li · Ying Wang ·
Chun Zhou · Weiwei Shao · Jin Peng ·
Yan You · Xinwen Zhang · Xiaoyan Shen

Received: 16 March 2013 / Accepted: 24 May 2013 / Published online: 6 June 2013
© Springer Science+Business Media New York 2013

Abstract Malignant gliomas (MGs) are among the most aggressive types of cancers in the human brain. Frequent tumor recurrence caused by a lack of effective therapeutic approaches results in a poor prognosis. Signal transducer and activator of transcription 3 (STAT3), an oncogenic protein, is constitutively activated in MGs and predicts a poor clinical outcome. STAT3 therefore is considered to be a promising target for the treatment of MGs. Cryptotanshinone (CTS), the main bioactive compound from the root of *Salvia miltiorrhiza* Bunge, has been reported to have various pharmacological effects. However, little is known about its function in MG cells. In this study, we evaluated the effect of CTS on the proliferation of human glioma cell lines (T98G and U87). Our results revealed that CTS significantly suppresses glioma cell proliferation. The phosphorylation of STAT3 Tyr705, but not Ser727, was inhibited by CTS, and STAT3 nuclear translocation was attenuated. Overexpression of constitutively active mutant STAT3C reversed the inhibitory effect of CTS, while knockdown STAT3 showed a similar inhibitory effect as CTS treatment. Following the downregulation of STAT3-regulated proteins cyclinD1 and survivin, cell cycle progression significantly arrested in G1/G0 phase. These results indicate that CTS may be a potential antiproliferation agent for the treatment of MGs and that its mechanism may be related to the inhibition of STAT3 signaling.

Keywords Cryptotanshinone · Proliferation · Signal transducer and activator of transcription 3 · Malignant gliomas

Introduction

Malignant gliomas (MGs) are the most common malignancy in primary brain tumors and have a high mortality [1, 2]. Classical therapeutic approaches for MGs include surgical resection, post-operative radiotherapy, and chemotherapy (usually with temozolomide). However, based on these therapies, the median survival time is only 14.6 months, and the survival rate has not shown significant improvement in the last two decades [3, 4]. The exploration of more effective therapeutic approaches is therefore necessary for improving the outcome of glioma treatment.

It has been reported that several signaling pathways are abnormally activated in gliomas genesis, such as phosphatidylinositol-3'-kinase (PI3K)/Akt, Mammalian target of rapamycin (mTOR), Ras/Extracellular signal regulated kinase (Erk), and Janus kinase (JAK)2/signal transducer and activator of transcription 3 (STAT3) signaling pathways [5–7]. In recent years, as a master transcription factor as well as an oncogenic protein, it has been reported that STAT3 plays a key role in the signaling pathways involved in the transition from low- to high-grade glioma [8]. STAT3 has been reported to be constitutively activated and indicates a poor clinical prognosis in MGs [9, 10]. When STAT3 is activated upon phosphorylation of the tyrosine705 residue, monomeric STAT3 forms dimers through their SH2 domains and translocates from the cytoplasm to the nucleus. Once reaching there, STAT3 transcriptionally regulates the expression of its target genes, such as cyclin

L. Lu · C. Li · D. Li · Y. Wang · C. Zhou · W. Shao · J. Peng ·
Y. You · X. Zhang · X. Shen (✉)
Laboratory of Pharmacology and Toxicology,
School of Pharmaceutical Science, Sun Yat-Sen University,
Guangzhou 510006, China
e-mail: shxiaoy@mail.sysu.edu.cn

D1, survivin, mcl-1, Vascular endothelial growth factor receptor (VEGF), Matrix Metalloproteinase (MMP)-2, MMP-9, etc. The activation of these genes gives STAT3 a direct role in cancer survival, proliferation, apoptosis, angiogenesis, invasion, and metastasis [11]. Thus, STAT3 signaling has been considered as a potential target for therapeutic intervention for MGs [9, 12].

Cryptotanshinone (CTS), which is the one of the major representative components isolated from the root of *Salvia miltiorrhiza* Bunge, has been reported to have various pharmacological effects. It has been reported that CTS attenuated oxidized low-density lipoprotein-induced prelesional atherosclerotic events, and attenuated the injury of rat myocardial ischemia/reperfusion in vivo [13, 14]. In RAW264.7 cells, CTS suppressed the secretion of inflammatory cytokines by inhibiting the NF- κ B and Mitogen-activated protein kinase (MAPK) signaling pathways [15]. CTS was also reported to modulate the metabolism of amyloid precursor protein resulting in neuroprotection and anti-Alzheimer disease function [16]. An antitumor activity for CTS has also been found in several studies [17–22]. However, until now, little is known about the effect of CTS in MGs. In the present study, we determined the effects of CTS on human glioma cells. For the first time, we show that CTS suppresses the proliferation of the human malignant glioma cell lines T98G and U87 through inhibition of the STAT3 signaling pathway. Our results provide evidence for CTS as a potential therapeutic agent for MGs.

Materials and methods

Materials

CTS, 3-(4, 5-dimethylthiazol-2-yl)-2, 5-diphenyltetrazolium bromide (MTT), and dimethyl sulfoxide (DMSO) were obtained from Sigma Aldrich (St. Louis, MO, USA). Dulbecco's modified Eagle's medium (DMEM) and fetal bovine serum (FBS) were obtained from Invitrogen-Gibco (Grand Island, NY, USA). The BrdU Cell Proliferation Assay was obtained from Exalpha Biologicals (Shirley, MA, USA). Anti-phospho-STAT3 (Tyr705) and anti-phospho-JAK2 antibodies were purchased from Epitomics (Burlingame, CA, USA). Anti-STAT3, anti-phospho-STAT3 (Ser727), anti-phospho-p44/42 Erk1/2 (Thr202/Tyr204), anti-phospho-mTOR (Ser2448), and anti-phospho-Akt antibodies were purchased from Cell Signaling Technology, Inc., (San Francisco, CA, USA). The anti-GAPDH antibody was from Beyotime (Suzhou, Jiangsu, China). STAT3C plasmid was obtained from Addgene plasmid repository [22]. STAT3 Small Interfering RNA (siRNA) was purchased from Shanghai Genepharma Co., (Shanghai, China). The sequence for STAT3 were as

follows: Sense, 5'-UGUUCUCUGAGACCCAUGAdTdT-3'; Antisense, 5'-UCAUGGGUCUCAGA GACAdTdT-3' [21]. The sequence for negative control (NC) were as follows: Sense, 5'-UUCUCCGAACGUGUCACGUTT-3'; Antisense, 5'-ACGUGACACGUUCGGA GAATT-3'.

Cell culture

T98G and U87 cells were from the China Center for Type Culture Collection of the Chinese Academy of Sciences. Cells were cultured and maintained in high-glucose Dulbecco's modified Eagle's medium (DMEM) supplemented with 10 % (v/v) fetal bovine serum (FBS), 100 μ g of streptomycin/ml, and 100 U of penicillin/ml, and incubated at 37 °C with a 5 % CO₂ humidified atmosphere. Stock cultures were routinely subcultured at 1:5 ratio at a weekly interval.

MTT assay

To measure cell growth, MTT assays were performed. Cells were plated in 100 μ l of medium/well in 96-well plates. After incubation overnight, cells were treated with various concentrations of CTS for 24–48 h, followed by MTT (5 mg/ml) incubation and DMSO (100 μ l/well) dissolution. Absorbance at 570 nm was measured using an automated microplate reader (Bio-Tech, Winooski, VT, USA).

BrdU cell proliferation assay

Cell proliferation was evaluated using BrdU cell proliferation assay kits according to the manufacturer's instructions with slight modification. In brief, cells suspended in growth medium were seeded in a 96-well plate at a density of 1×10^4 cells/well and grown overnight at 37 °C in a humidified incubator with 5 % CO₂. The next day, CTS (0–20 μ M) was added. After incubation for 48 h, 20 μ l of BrdU was added to each well, and the cells were incubated for 12 h. Fixing solution was then added and incubated for 30 min at room temperature. After washing, cells were incubated with a prediluted detector antibody for 1 h at room temperature. Acid stop solution was added after incubation with HRP-conjugated secondary antibody for 1 h at room temperature. The optical density (OD) was then measured at 450 nm using an automated microplate reader.

Western blotting

Cells from different experimental conditions were washed twice with ice-cold PBS and lysed in either RIPA buffer (50 mM Tris, pH 7.4, 150 mM NaCl, 1 mM PMSF, 1 mM

EDTA, 1 % Triton X-100, 0.1 % sodium dodecyl sulfate (SDS), 1 mM Na₃VO₄, 1 mM NaF, and protease inhibitor cocktail (Roche Diagnostics Ltd, Mannheim, Germany)) or sample buffer (62.5 mM Tris–HCl pH 6.8, 2 % (w/v) SDS, 10 % glycerol, 5 % β-mercaptoethanol, and 0.1 % (w/v) bromophenol blue). Samples with equal amounts of protein were separated by SDS-PAGE gel electrophoresis and transferred to nitrocellulose membranes (Millipore, Bedford, MA, USA). The membranes were blocked with 5 % nonfat milk in PBS containing 0.05 % Tween-20 for 1 h, followed by incubation with the primary antibody overnight at 4 °C. The membranes were then washed and incubated with horseradish peroxidase-conjugated secondary antibody for 1 h at room temperature. Immunoreactive bands were detected by enhanced chemiluminescence and visualized from the Image on Quant Las 4000 (GE Healthcare, Piscataway, NJ, USA).

Immunofluorescence staining

T98G and U87 cells were treated with 10 μM CTS for 2 h. Control cells were incubated with vehicle only (DMSO) at a concentration equal to that in drug-treated cells (final concentration 0.1 %). Cells were fixed with 4 % paraformaldehyde in PBS buffer (30 min, room temperature), blocked for 1 h with 10 % normal goat serum containing 0.1 % saponin for permeabilization, and incubated with primary antibodies diluted in blocking buffer, STAT3 or p-STAT3 (Tyr705) diluted 1:100 overnight at 4 °C. After

washing with PBS, cells were incubated with Alexa 488 Fluor-labeled secondary antibodies (diluted 1:1,000 in blocking buffer) for 1 h and washed with PBS. Coverslips were mounted in Prolong Gold antifade reagent with DAPI (Molecular Probes, Eugene, OR, USA) and inspected with a confocal microscope Zeiss 710 (Zeiss, Jena, Thuringia, Germany).

Transfections

STAT3C transfection was performed by nucleofection system (Amaxa, Koeln, Germany) with Amaxa cell line nucleofector kit T according to the manufacturer's instructions. STAT3 siRNA was transfected using lipofectamine 2000 (Invitrogen, Carlsbad, CA) according to the manufacturer's instructions. Overexpression STAT3C and STAT3 siRNA were verified by western blotting. After transfected for 48 h, total cell lysates were collected and analyzed for STAT3 and STAT3-regulated proteins (cyclinD1, survivin).

Flow cytometry

Cells were seeded in 35-mm dishes at a density of 4×10^5 cells/dish in culture medium and grown overnight at 37 °C in a humidified incubator with 5 % CO₂. After treatment with CTS (0–20 μM) for 24 h, the cells were briefly washed with PBS and trypsinized. Cell suspensions were centrifuged at 1,000 rpm for 3 min, fixed with ice-cold ethanol (70 %, v/v) overnight at 4 °C, and stained with PI

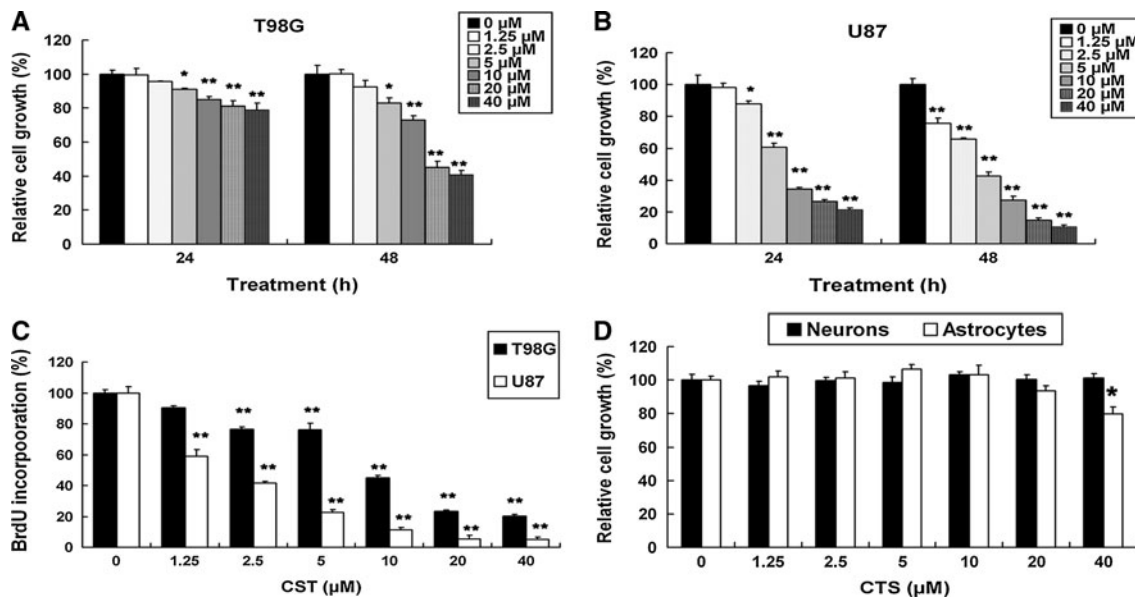


Fig. 1 Effects of CTS on proliferation of T98G and U87 cells. **a**, **b**, and **d** T98G, U87, and normal cells (primary rat cortical neuron and astrocyte) were treated with different doses of CTS (0–40 μM) for the indicated time. Cell growth was measured by MTT assay. **c** The

proliferation of T98G and U87 cells treated with different doses of CTS for 48 h was measured by BrdU cell proliferation assay. Data are expressed as mean ± SEM $n = 3$ for each group. * $P < 0.05$, ** $P < 0.01$ versus control group

(50 $\mu\text{g/ml}$) in sample buffer containing RNaseA (100 U/ml) for 30 min at room temperature. The percentage of cells within each phase of the cell cycle (G0/G1, S, or G2/M) was determined by flow cytometer (Becton–Dickinson, Mountain View, CA, USA).

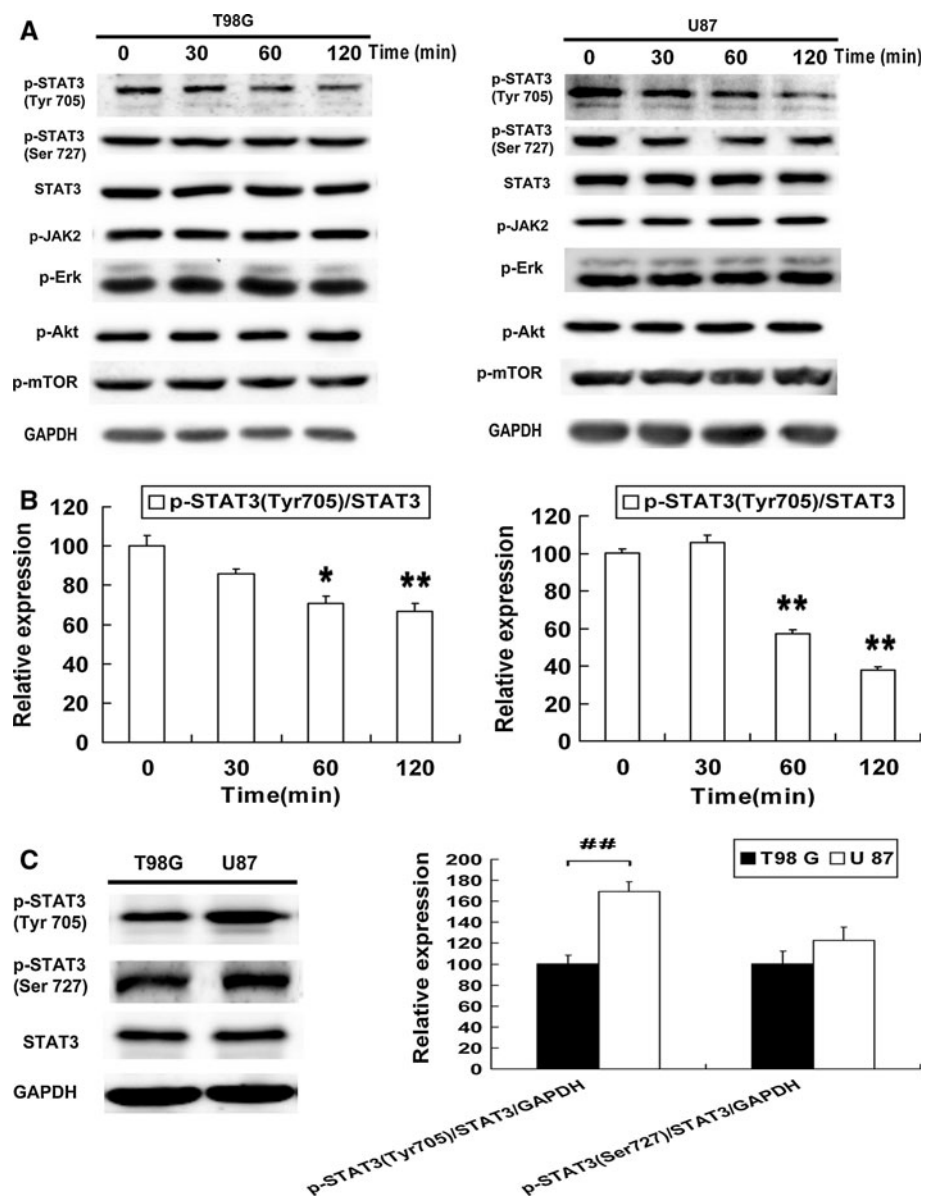
Statistical analysis

All of the described experiments were performed more than three times, and the data were expressed as means \pm standard error of the mean (SEM). The statistical difference between two experimental groups was determined using an independent-samples *t* test, and differences among the groups were assessed by one-way ANOVA and LSD post-hoc test. Results were analyzed using SPSS 13.0 software (SPSS Inc., Chicago, IL, USA).

Fig. 2 CTS inhibits the phosphorylation of STAT3 at Tyr705. Effects of CTS on phosphorylation of STAT3 Tyr705, Ser727, JAK-2, Erk, Akt, and mTOR were determined by western blotting. **a** CTS (10 μM) inhibited the phosphorylation of STAT3 Tyr705 in a time-dependent manner in T98G and U87 cells. In addition, CTS treatment for 2 h inhibited the phosphorylation of STAT3 Ser727 slightly in U87 cells but not in T98G cells. **b** Relative protein expression of p-STAT3 Tyr705 was quantified by densitometry. Data are expressed as mean \pm SEM $n = 3$ for each group. * $P < 0.05$, ** $P < 0.01$ vs control group. **c** *Left*: comparison of the levels of STAT3, p-STAT3 (Tyr705), and p-STAT3 (Ser727) between T98G and U87 cells under normal culture conditions. *Right*: relative protein expression was quantified by densitometry. Data are expressed as mean \pm SEM $n = 3$ for each group. # $P < 0.05$, ## $P < 0.01$, significant difference between groups

Results

The effect of CTS on the proliferation of T98G and U87 cells was measured by MTT assay. As shown in Fig. 1a, b, CTS inhibited the rate of cell growth in a time- and a concentration-dependent manner in both T98G and U87 cells. To confirm the inhibitory effect of CTS on cell proliferation, a BrdU incorporation assay was used. As shown in Fig. 1c, CTS inhibited BrdU incorporation in T98G and U87 cells in a dose-dependent manner. These results indicate that CTS has antiproliferative activity in glioma cells and U87 cells are more sensitive to CTS than T98G cells. Furthermore, to confirm whether CTS is toxic to all culture cells, normal cells (primary rat cortical neuron and astrocyte) were treated with CTS for 48 h. CTS, at a concentration range of 1.25–20 μM , was not toxic to



normal cells. CTS at 40 μM induced a significant reduction in astrocyte cell growth (Fig. 1d).

STAT3 signaling pathway plays a pivotal role in tumor growth [8], and human glioma cells are known to express constitutively active STAT3 [9]. Therefore, we explored whether CTS had an effect on the constitutively active STAT3 in T98G and U87 cells. As shown in Fig. 2a, b, CTS (10 μM) inhibited phosphorylation of STAT3 at Tyr705 in a time-dependent manner in T98G cells, but had no effect on the phosphorylation of Ser727 or total STAT3 protein. However, in U87 cells, CTS (10 μM) not only inhibited the phosphorylation of STAT3 at Tyr705 in a time-dependent manner but also inhibited the phosphorylation of Ser727 slightly. To explore which signal pathway caused the inhibition of STAT3 Tyr705 phosphorylation, some upstream kinases of STAT3, especially those with close relation to cell proliferation, including phosphorylated JAK2, Erk, Akt, and mTOR, were also detected. However, the phosphorylations of them were not affected by CTS. Furthermore, we compared the differences of the basal phosphorylation levels of STAT3 between the two cell lines. We found that the basal level of p-STAT3 (Tyr705) in U87 cells was much higher than that in T98G cells (Fig. 2c). To confirm the effect of STAT3 signaling inhibition by CTS, the cellular location of STAT3 was stained in T98G and U87 cells. As shown as in Fig. 3a, in

normal condition (control cell), STAT3 prominently located in nucleus. After being stimulated with CTS for 2 h, STAT3 nuclear translocation was attenuated, with STAT3 being mainly located in cytoplasm. To confirm the result of inhibition of p-STAT3 (Tyr705), we also stained p-STAT3 (Tyr705) and also observed by confocal microscopy. As expected in Fig. 3b, in normal condition (control cell), the expression of p-STAT3 (Tyr705) was concentrated mainly in the nucleus. After CTS treatment, p-STAT3 (Tyr705) was diminished dramatically in the nucleus.

To explore which cell cycle phase CTS affected, flow cytometry analysis was used. As shown in Fig. 4a, b, 20 μM CTS significantly increased the proportion of T98G cells in G1/G0 phase from 61.7 to 79.9 %. The increased G1/G0 cell population was accompanied by a concomitant decrease in the number of cells in S phase and G2/M phase of the cell cycle. The inhibitory effect of CTS on cell cycle progression in U87 cells was stronger than in T98G cells. CTS treatment at 10 and 20 μM significantly increased the proportion of T98G cells in G1/G0 phase from 50.5 to 70.7 % and from 50.5 to 79.7 %, respectively. These results were consistent with the results from Fig. 1c. To further explore the expression of STAT3-regulated proteins which are involved in the cell cycle (Fig. 4c), we examined the expression of cyclin D1 and survivin after CTS treatment. In T98G cells, CTS at 5 and 10 μM downregulated

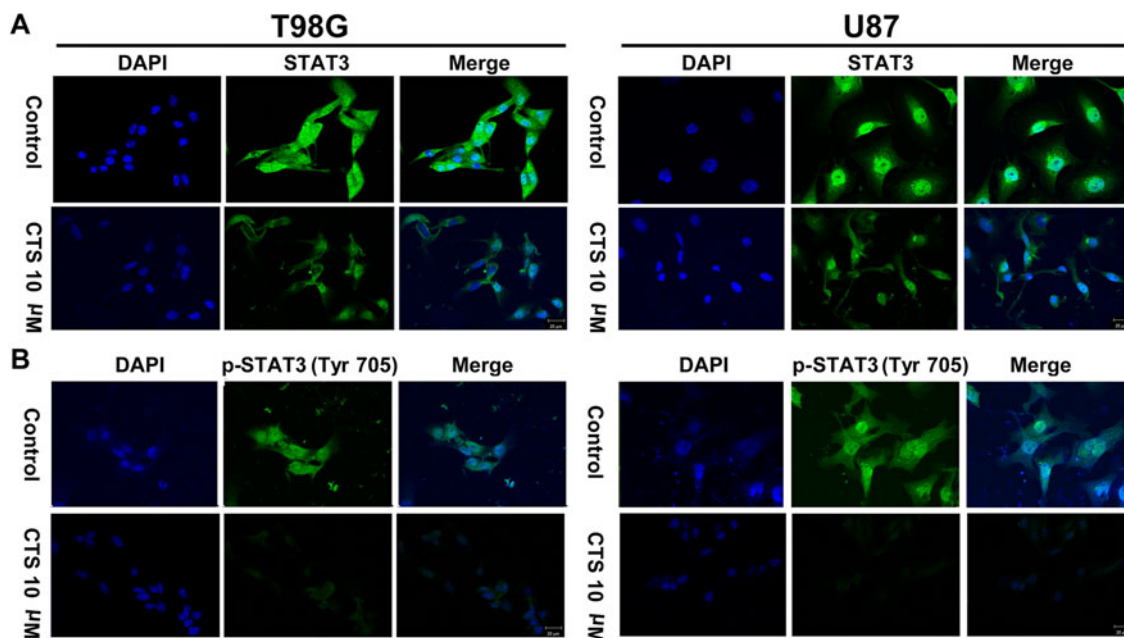


Fig. 3 CTS inhibits G1/S cell cycle progression in glioma cells and downregulates STAT3-regulated proteins expression. **a** Representative results of cell cycle analysis in T98G or U87 cells treated with different doses of CTS. **b** The G0/G1, S, and G2/M fractions were measured. Data are expressed as mean \pm SEM $n = 3$ for each group. * $P < 0.05$, ** $P < 0.01$ versus control group. **c** Cells were treated

with CTS at the indicated concentrations for 24 h. Proteins were analyzed by western blotting with specific antibodies. CTS suppressed the expression of cyclin D1, and survivin in T98G and U87 cells. Relative protein expression was quantified by densitometry. Data are expressed as mean \pm SEM $n = 3$ for each group. * $P < 0.05$, ** $P < 0.01$ versus control group

cyclin D1 protein expression, but the difference was not significant when compared with control cells. However, significant inhibition did occur with 20 μM CTS treatment. The expression level of cyclin D1 was decreased by 37.39 % ($P < 0.05$), and survivin protein expression was suppressed in a dose-dependent manner. In U87 cells, CTS suppressed the expression of cyclin D1 and survivin in a dose-dependent manner, and the maximum inhibitions were 54 % ($P < 0.01$), 36.09 % ($P < 0.01$), respectively. These results indicate that CTS downregulated the expression of STAT3 target proteins in both T98G and U87 cells.

To find out whether the antiproliferation function of CTS was induced by specific inhibition of STAT3 Tyr705 phosphorylation, STAT3C, which keeps dimerizing and being constitutively active but without tyrosine phosphorylation and which has been used in previous studies [23–25], was transfected in T98G and U87 cells. Comparing with Mock-transfected control cells, gliomas cell transfected with STAT3C presented a significant increase in cell growth after treatment with CTS at 5–20 μM (Fig. 5a, b, left). Enforced expression of STAT3C in T98G and U87 was verified by western blot. Comparing with mock-transfected control cells, the expression of STAT3 was increased. Consistent with that, STAT-regulated proteins cyclinD1 and survivin were also increased (Fig. 5a, b, right). In order to know the connection between cell proliferation and STAT3 signaling in gliomas, STAT3 siRNA was transfected in T98G and U87 cells. Comparing with NC-transfected cells, gliomas cell transfected with STAT3 siRNA showed a significant inhibition in cell proliferation (Fig. 5c, left). Knockdown STAT3 in T98G and U87 was verified by western blot. Comparing with NC-transfected cells, the expression of STAT3 protein was decreased. Consistent with that, STAT3-regulated proteins cyclinD1 and survivin were also decreased (Fig. 5c, right).

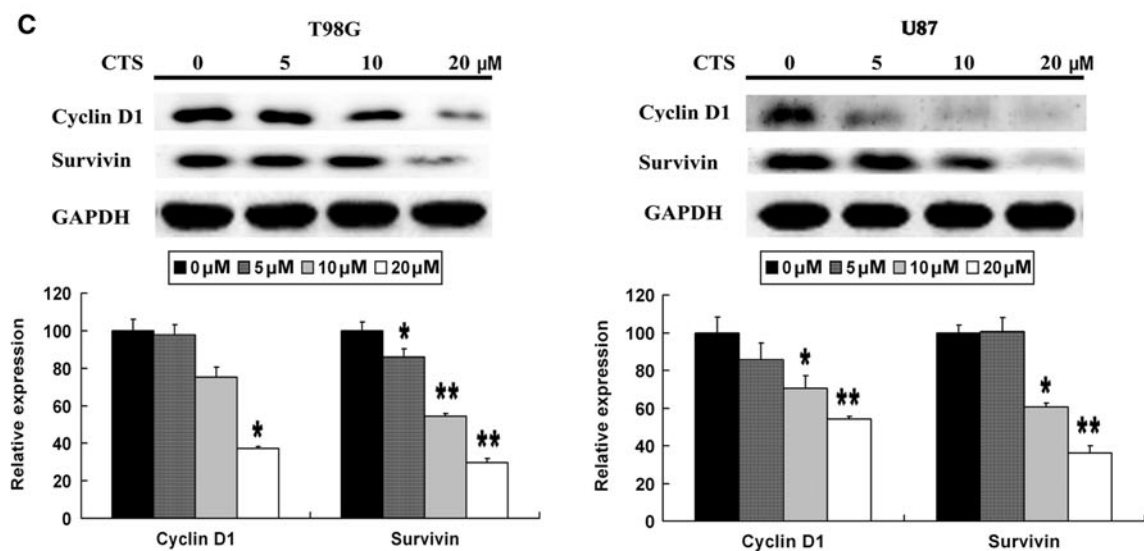
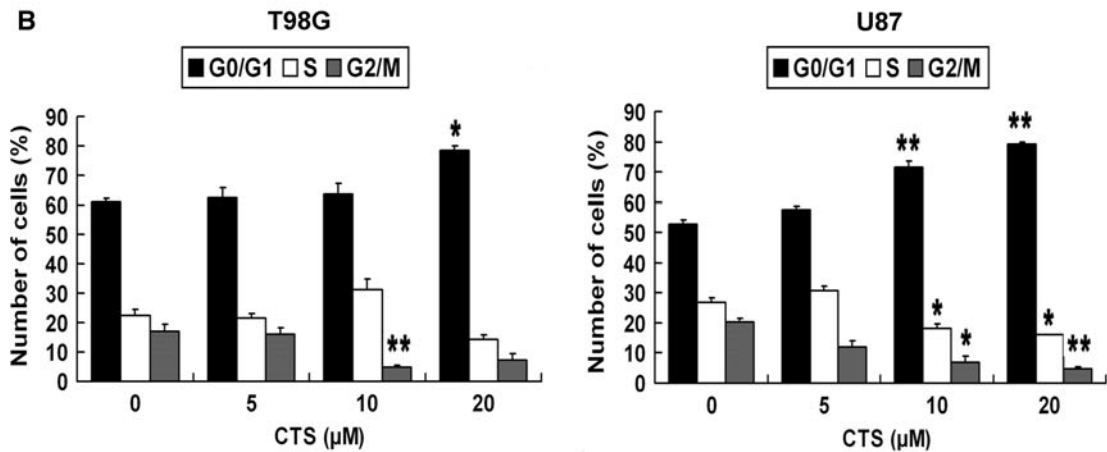
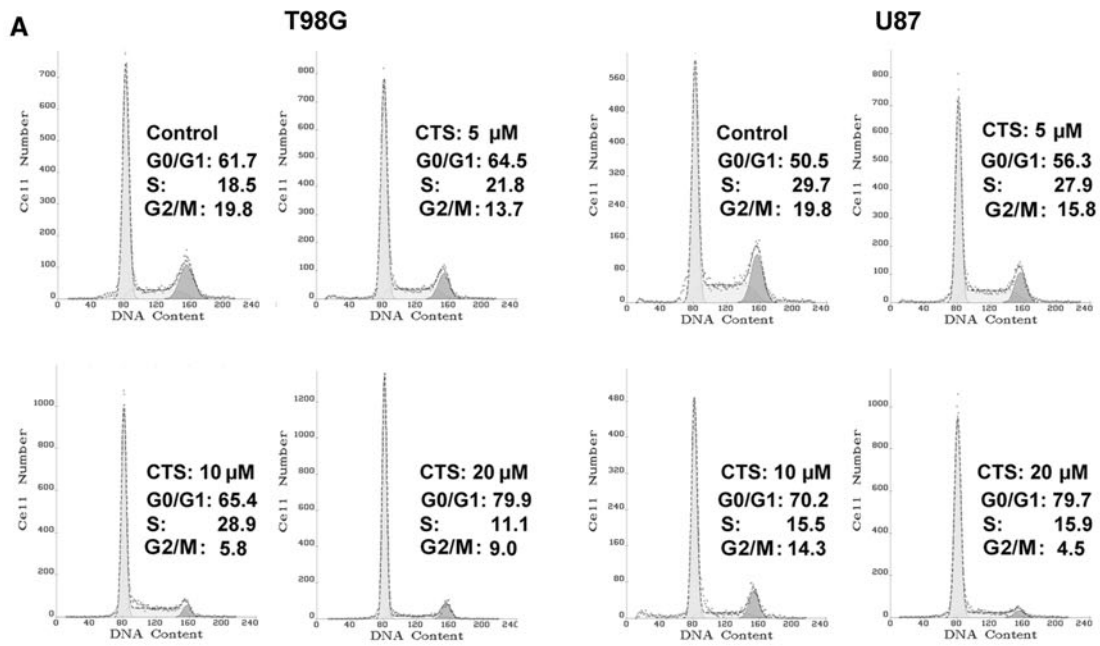
Discussion

In this study, we examined role of CTS in glioma cell proliferation and explored its potential mechanism. Our results showed that (1) CTS inhibits glioma cell proliferation. In a large range of treatment concentrations, CTS is nontoxic to normal cells in the range of effective dosage. (2) CTS specifically inhibits the phosphorylation of STAT3 at Tyr705. Enforced expression of constitutively active mutant STAT3C reverses gliomas from CTS-induced inhibitory effect, while knockdown STAT3 inhibits glioma cell proliferation. (3) CTS arrests cell cycle progression in G1/G0 phase and downregulates STAT3-regulated proteins cyclinD1 and survivin.

Although the antitumor activity of CTS has been previously described [17–22], our study is the first to explore

Fig. 4 The effect of CTS on STAT3 location, phosphorylation of STAT3 Tyr705 by Immunofluorescence staining. T98G and U87 cells were treated with CTS 10 μM for 2 h. **a** Representative confocal immunofluorescent analysis of T98G and U87 cells using STAT3 antibody (green). **b** Representative confocal immunofluorescent analysis of T98G and U87 cells using p-STAT3 (Tyr705) antibody (green). After CTS 10 μM treatment, the expression of p-STAT3 (Tyr705) was weaker. DAPI (blue) was used to counterstain the cell nuclei. Bar = 20 μm

the effect of CTS on human glioma cells. In HepG2 and MCF7 cancer cells, CTS inhibits cell growth by inducing apoptosis [17]. In prostate cancer, leukemia and hela cell lines, CTS induces cell growth by both inducing apoptosis and inhibition of proliferation [18–21]. We found CTS inhibits proliferation in glioma cells, and there is no evidence to show CTS induces apoptosis (Data not shown). More important, CTS is nontoxic in normal cells, except for a minor decrease in astrocytic viability at 40 μM , which is hard to achievable concentrations in vivo [26]. Thus, CTS probably don't cause adverse affect on normal brain. In fact, CTS is neuroprotective in AD animal model [16]. Since STAT3 is constitutively activated in MGs, but not in normal cell, specific targeting of STAT3 signaling is considered a potential therapeutic approach for MGs [9]. Thus, the molecular basis for the tumor-specific actions of CTS may be dependent on the basal level of activated STAT3 (p-STAT3 Tyr705). Comparing the inhibitory effect of CTS in T98G and U87 cell, we found that U87 cells were more sensitive to CTS inhibition (Fig. 1c). CTS inhibited p-STAT3 (Tyr705) in a time-dependent manner in both T98G and U87 cells, and effected a minor inhibition of p-STAT3 (Ser727) in U87 but not in T98G cells (Fig. 2a, b). Then, we compared the basal level of STAT3 and found that the level of phosphorylated STAT3 Tyr705 in U87 cell was higher than that in T98G (Fig. 2c). Hence, the data imply that higher basal level of activated STAT3 correlates with stronger inhibition by CTS and explains why CTS treatment is more sensitive in U87 cells than in T98G. Furthermore, we designed STAT3C rescue test to prove the role of p-STAT3 (Tyr705) (Fig. 4). Meanwhile, some major pathways contribute to activating STAT3: cytokine, growth factors stimulation of membrane receptors (IL-6, epidermal growth factor, and platelet-derived growth factor receptors, etc.) or nonreceptor tyrosine kinas (Src), and then activation of downstream kinases, such as JAK2, Akt, Erk, and mTOR [5, 6, 11, 27, 28]. it has previously been reported that CTS did not affect the phosphorylation of upstream kinases, such as EGFR and Src [21]. Hence, in our study, we chose to detect the downstream kinases of these growth factors and cytokine receptors activation, which are also abnormally activated in gliomas genesis: p-Akt, Erk, mTOR, and JAK2 [5–7]. Unfortunately, we did not find any alternation of p-Akt, Erk, mTOR, and JAK2 (Fig. 2a, b). Although recent studies have shown that CTS inhibits



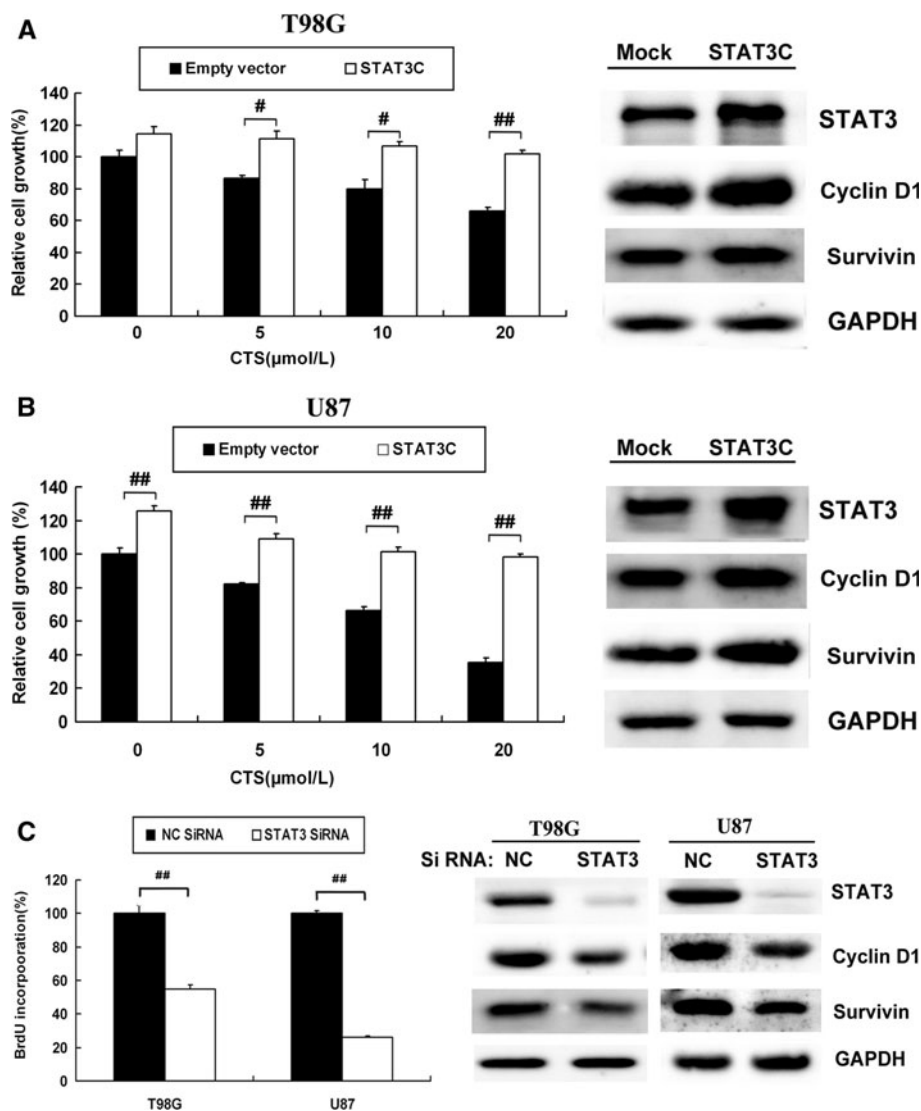


Fig. 5 Effect of constitutively active mutant STAT3C or STAT3 siRNA on glioma cell proliferation **a** and **b** *Left*: T98G and U87 cell were transfected with mock-(empty vector) or STAT3C plasmid for 24 h, and then treated with CTS at the indicated concentrations for another 24 h. Cell growth was measured by MTT assay. Vehicle-treated cells were used as a control. Data are expressed as a percentage vs. control (100 %). Data are expressed as mean \pm SEM $n = 3$ for each group. $^{\#}P < 0.05$, $^{\#\#}P < 0.01$, significant difference between groups. *Right*: Mock- or STAT3C- transfected T98G and U87 cells were harvested after 48 h. Proteins were analyzed by western blotting with specific antibodies of STAT3 and STAT3-

regulated proteins cyclin D1 and survivin. **c** *Left*: T98G and U87 cells were transfected with NC and STAT3 SiRNA for 48 h. Cell proliferation was measured by BrdU cell-proliferation assay. NC-transfected cells were used as a control. Data are expressed as a percentage vs. control (100 %). Data are expressed as mean \pm SEM $n = 3$ for each group. $^{\#}P < 0.05$, $^{\#\#}$ significant difference between groups. *Right*: NC or STAT3 SiRNA transfected T98G and U87 cells were harvested after 48 h. Proteins were analyzed by western blotting with specific antibodies of STAT3 and STAT3-regulated proteins cyclin D1 and survivin

proliferation of Rh30 and DU145 through inhibiting mTOR signaling, it had previously been reported that CTS inhibits p-Akt during C5a-induced migration of RAW264.7 macrophages [22, 29]. Therefore CTS may have different effects and mechanisms in different cell types. Take together, we confirm that CTS specifically blocks the tyrosine phosphorylation of STAT3.

Cell proliferation is closely related to cell cycle progression. Consistent with that, STAT3-regulated proteins

which are related to cell cycle progression were down-regulated by CTS. As shown in Fig. 4a, b, CTS arrests cell cycle progression in G1/G0 phase. In order to know the downstream factors of STAT3 signaling on cell proliferation, we detected the effect of CTS on STAT3-regulated proteins cyclin D1 and survivin, which are highly expressed in MGs. These two proteins are strong cell cycle regulators: cyclinD1 is essential for promoting G1/S progression in human tumor cell lines; survivin, one of the

inhibitors of apoptosis proteins family (IAPs), is closely related with both S- and G2/M-phase progressions [30–33]. As we expected, the expressions of cyclin D1 and survivin were decreased by CTS. Furthermore, STAT3 knockdown indeed inhibits cell proliferation of gliomas cells (Fig. 5c) and downregulated the expressions of cyclin D1 and survivin. Our data indicate that the antiproliferation effect of CTS might be related to inhibiting the expression of STAT3-regulated proteins such as cyclin D1 and survivin.

In summary, the present study demonstrates that CTS may be a potential antiproliferative therapeutic candidate for glioma treatment, and its mechanism may be related to the inhibition of STAT3 signaling.

Acknowledgments This study was supported by the National Natural Science Foundation of China (No. 31070924 and 81173056), Projects of International Cooperation and Exchanges, Science and Technology Planning Project of Guangdong Province, China (No. 1011420600004), and the Research Fund for the Doctoral Program of Higher Education of China (No. 20100171110052).

References

- Ohgaki H, Kleihues P (2005) Population-based studies on incidence, survival rates, and genetic alterations in astrocytic and oligodendroglial gliomas. *J Neuropathol Exp Neurol* 64:479–489
- Dolecek TA, Propp JM, Stroup NE, Kruchko C (2012) CBTRUS statistical report: primary brain and central nervous system tumors diagnosed in the United States in 2005–2009. *Neuro Oncol* 14:v1–v49
- Stupp R, Mason WP, van den Bent MJ et al (2005) Radiotherapy plus concomitant and adjuvant temozolomide for glioblastoma. *N Engl J Med* 352:987–996
- Deorah S, Lynch CF, Sibenaller ZA, Ryken TC (2006) Trends in brain cancer incidence and survival in the United States: surveillance, epidemiology, and end results program, 1973–2001. *Neurosurg Focus* 20:E1
- Lo HW (2010) Targeting Ras-RAF-ERK and its interactive pathways as a novel therapy for malignant gliomas. *Curr Cancer Drug Targets* 10:840–848
- Herbert B Newton (2004) Molecular neuro-oncology and development of targeted therapeutic strategies for brain tumors. Part 2: p13K/Akt/PTEN, mTOR, SHH/PTCH and angiogenesis 4:105–128
- Stechishin OD, Luchman HA, Ruan Y et al (2013) On-target JAK2/STAT3 inhibition slows disease progression in orthotopic xenografts of human glioblastoma brain tumor stem cells. *Neuro Oncol* 15:198–207
- Doucette TA, Kong LY, Yang Y et al (2012) Signal transducer and activator of transcription 3 promotes angiogenesis and drives malignant progression in glioma. *Neuro Oncol* 14:1136–1145
- Heimberger AB, Priebe W (2008) Small molecular inhibitors of p-STAT3: novel agents for treatment of primary and metastatic CNS cancers. *Recent Pat CNS Drug Discov* 3:179–188
- Carro MS, Lim WK, Alvarez MJ et al (2010) The transcriptional network for mesenchymal transformation of brain tumours. *Nature* 463:318–325
- Huang S (2007) Regulation of metastases by signal transducer and activator of transcription 3 signaling pathway: clinical implications. *Cancer Res* 13:1362–1366
- Heimberger AB (2011) The therapeutic potential of inhibitors of the signal transducer and activator of transcription 3 for central nervous system malignancies. *Surg Neurol Int* 2:163
- Ang KP, Tan HK, Selvaraja M et al (2011) Cryptotanshinone attenuates in vitro oxLDL-induced pre-lesional atherosclerotic events. *Planta Med* 77:1782–1787
- Jin YC, Kim CW, Kim YM et al (2009) Cryptotanshinone, a lipophilic compound of *Salvia miltiorrhiza* root, inhibits TNF- α -induced expression of adhesion molecules in HUVEC and attenuates rat myocardial ischemia/reperfusion injury in vivo. *Eur J Pharmacol* 614:91–97
- Tang S, Shen XY, Huang HQ et al (2011) Cryptotanshinone suppressed inflammatory cytokines secretion in RAW264.7 macrophages through inhibition of the NF- κ B and MAPK signaling pathways. *Inflammation* 34:111–118
- Mei Z, Zhang F, Tao L et al (2009) Cryptotanshinone, a compound from *Salvia miltiorrhiza* modulates amyloid precursor protein metabolism and attenuates beta-amyloid deposition through upregulating alpha-secretase in vivo and in vitro. *Neurosci Lett* 452:90–95
- Park JJ, Kim MJ, Park OJ et al (2012) Cryptotanshinone induces ER stress-mediated apoptosis in HepG2 and MCF7 cells. *Apoptosis* 17:248–257
- Gong Y, Li Y, Lu Y et al (2011) Bioactive tanshinones in *Salvia miltiorrhiza* inhibit the growth of prostate cancer cells in vitro and in mice. *Int J Cancer* 129:1042–1052
- Li H, Zhang Q, Chu T et al (2012) Growth-inhibitory and apoptosis-inducing effects of tanshinones on hematological malignancy cells and their structure-activity relationship. *Anti-cancer Drugs* 23:846–855
- Ye Y, Xu W, Zhong W (2010) Effects of cryptotanshinone on proliferation and apoptosis of HeLa cell line of cervical cancer. *Zhongguo Zhong Yao Za Zhi* 35:118–121
- Shin DS, Kim HN, Shin KD (2009) Cryptotanshinone inhibits constitutive signal transducer and activator of transcription 3 function through blocking the dimerization in DU145 prostate cancer cells. *Cancer Res* 69:193–202
- Chen W, Luo Y, Liu L et al (2010) Cryptotanshinone inhibits cancer cell proliferation by suppressing Mammalian target of rapamycin-mediated cyclin D1 expression and Rb phosphorylation. *Cancer Prev Res (Phila)* 3:1015–1025
- Bromberg JF, Wrzeszczynska MH, Devgan G et al (1999) Stat3 as an oncogene. *Cell* 98:295–303
- Hillion J, Dhara S, Sumter TF et al (2008) The high-mobility group A1a/signal transducer and activator of transcription-3 axis: an achilles heel for hematopoietic malignancies? *Cancer Res* 68:10121–10127
- Weissenberger J, Priester M, Bernreuther C et al (2010) Dietary curcumin attenuates glioma growth in a syngeneic mouse model by inhibition of the JAK1,2/STAT3 signaling pathway. *Clin Cancer Res* 16:5781–5795
- Pan Y, Bi HC, Zhong GP et al (2008) Pharmacokinetic characterization of hydroxypropyl-beta-cyclodextrin-included complex of cryptotanshinone, an investigational cardiovascular drug purified from Danshen (*Salvia miltiorrhiza*). *Xenobiotica* 38:382–398
- Zhou J, Wulfschlegel J, Zhang H et al (2007) Activation of the PTEN/mTOR/STAT3 pathway in breast cancer stem-like cells is required for viability and maintenance. *Proc Natl Acad Sci USA* 104:16158–16163
- Rane SG, Reddy EP (2000) Janus kinases: components of multiple signaling pathways. *Oncogene* 19:5662–5679
- Don MJ, Liao JF, Lin LY, Chiou WF (2007) Cryptotanshinone inhibits chemotactic migration in macrophages through negative regulation of the PI3K signaling pathway. *Br J Pharmacol* 151:638–646
- Cavalla P, Dutto A, Piva R et al (1998) Cyclin D1 expression in gliomas. *Acta Neuropathol* 95:131–135
- Yamada Y, Kuroiwa T, Nakagawa T et al (2003) Transcriptional expression of survivin and its splice variants in brain tumors in humans. *J Neurosurg* 99:738–745

32. Stacey DW (2003) Cyclin D1 serves as a cell cycle regulatory switch in actively proliferating cells. *Curr Opin Cell Biol* 15:158–163
33. Suzuki A, Hayashida M, Ito T et al (2000) Survivin initiates cell cycle entry by the competitive interaction with Cdk4/p16 (INK4a) and Cdk2/cyclin E complex activation. *Oncogene* 19:3225–3234